Inorg. Chem. **2002**, *41*, 6038–6047

Mononuclear Ca(II)–Bulky Aryl–Phosphate Monoanion and Dianion Complexes with Ortho-Amide Groups

Akira Onoda, Yusuke Yamada, Taka-aki Okamura, Hitoshi Yamamoto, and Norikazu Ueyama*

Department of Macromolecular Science, Graduate School of Science, Osaka University, Toyonaka, Osaka 560-0043 Japan

Received May 29, 2001

Two new mononuclear Ca(II) complexes with aryl dihydrogen phosphate ligands having two strategically oriented bulky amide groups, 2,6-$(Ph_3CCONH)_2C_6H_3OPO_3H_2$ (**1**), including one with a phosphate monoanion, $(NMe_4)[Ca^{II}\{O_2P(OH)OC_6H_3\text{-}2,6\text{-}(NHCOCPh_3)_2\}_3(N{\equiv}CMe)_3]$ (**3**), and one with a phosphate dianion, $[Ca^{II}\{O_3POC_6H_3\text{-}2,6\text{-}(NHCOCPh_3)_2\}(H_2O)_3(MeOH)_2]$ (**4**). Both are analogues for the NH···O hydrogen bonds in the active site of Ca(II)-containing phosphotransferase. Crystallographic studies of these Ca(II) complexes revealed that the amide NHs are directed to uncoordinated O atoms of the phosphates, and the IR and ^1H NMR spectra indicate that strong NH···O hydrogen bonds are formed only in the phosphate dianion state. The ligand exchange reaction of **3** with a non-hydrogen-bonded phosphate ligand shows that the NH···O hydrogen bonds prevent the Ca–O bond from dissociation. A scatter plot analysis comparing the distance of a Ca–O bond with the Ca–O–P angle, the Fourier density analysis, and DFT calculations reveal that a partial degree of covalency in the Ca–O(phosphate) bonds is present.

Introduction

Phosphotransferases containing both Ca(II) ion and hydrogen bonds provide catalytic activity for a variety of phosphoryl transfer reactions. The presence of both Ca(II) ions and hydrogen bonds acts to coordinate phosphate groups which are essential for their catalytic activity.[1,2] Most other phosphotransferases that contain different metal ions have a multinuclear metal center, while Ca(II)-containing phosphotransferases have a mononuclear core structure.[3] For example, in the active site of mammalian phosphoinositide specific phospholipase C, the phosphate groups coordinating to the Ca(II) ion have several NH···O hydrogen bonds with surrounding peptide NHs, as shown in Figure 1.[1] In the DNA molecule, the phosphate group from the main chain that coordinates to adjacent Ca(II) ions is also hydrogen-bonded with His NHs in deoxyribonuclease I.[4,5]

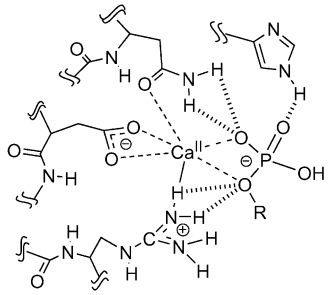

Figure 1. Active site of mammalian phosphoinositide specific phospholipase C.[1]

We have focused on the regulatory functions of NH···O hydrogen bonds to the phosphate groups in the Ca(II) coordination sphere. Our previous research showed that the dissociation of metal−carboxylate bonds was prevented by the coordination between NH···O hydrogen bonds and carboxylate groups, because the NH···O hydrogen bonds lower the pK_a value of the corresponding carboxylate.[6−9]

* To whom correspondence should be addressed. E-mail: ueyama@chem.sci.osaka-u.ac.jp.

(1) Essen, L.; Perisic, O.; Katan, M.; Wu, Y.; Roberts, M. F.; Williams, R. L. *Biochemistry* **1997**, *36*, 1704−1718.
(2) Ellis, M. V.; Katan, M. *Biochem. J.* **1995**, *213*, 339−347.
(3) Strater, N.; Lipscomb, W. N.; Klabunde, T.; Krebs, B. *Angew. Chem., Int. Ed. Engl.* **1996**, *35*, 2024−2055.
(4) Weston, S. A.; Lahm, A.; Suck, D. *J. Mol. Biol.* **1992**, *226*, 1237−1256.
(5) Oefner, C.; Suck, D. *J. Mol. Biol.* **1986**, *192*, 605−632.
(6) Ueyama, N.; Yamada, Y.; Takeda, J.; Okamura, T.; Mori, W.; Namakura, A. *J. Chem. Soc., Chem. Commun.* **1996**, 1377−1378.
(7) Yamada, Y.; Ueyama, N.; Okamura, T.; Mori, W.; Nakamura, A. *Inorg. Chim. Acta* **1998**, *275−276*, 43−51.
(8) Ueyama, N.; Takeda, J.; Yamada, Y.; Onoda, A.; Okamura, T.; Nakamura, A. *Inorg. Chem.* **1999**, *38*, 475−478.
(9) Ueyama, N.; Hosoi, T.; Yamada, Y.; Doi, M.; Okamura, T.; Nakamura, A. *Macromolecules* **1998**, *31*, 7119−7126.

10.1021/ic010570f CCC: $22.00
Published on Web 10/17/2002

Scheme 1. Novel Aryl Dihydrogen Phosphate Ligand with Bulky Amide Substituents in Ortho Positions.

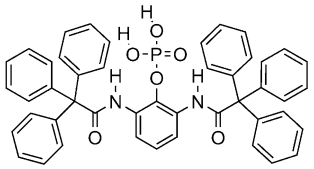

1

Because phosphoric acid groups have two dissociative protons with differing pK_a's, NH···O hydrogen bonds with them are thought to generate different distinctive properties as compared with carboxylic acid groups. Intermolecular NH···O hydrogen bonds in such phosphates have been found to be a functional component in the area of molecular recognition of acid/base catalysis.[10−15] In this study, we used NH-based functional analogues to investigate the relationship of the NH···O hydrogen bonds to the oxygen atoms of the phosphates that coordinate with Ca(II) complexes.

Extremely bulky amide aryldihydrogen phosphate ligands which can presumably enforce the mononuclear Ca(II) structures are newly designed for the detailed discussion of the hydrogen bonds and Ca−O bonds. For these analogues, we designed a novel aryl phosphate ligand having intramolecular NH···O hydrogen bonds, as shown in Scheme 1. Ca(II) complexes with phosphate ($ROPO_3$) and phosphonate ligands (RPO_3) are known to have polymeric structures, such as the one-dimensional structure of $Ca(O_3POCH_2CH_2NH_3)$[16−19] and the layered structure of $Ca(O_3PMe)$.[20−23] However, our designed amide ligands create bulkiness around the metal center which disrupts the formation of the polymeric coordination of Ca(II) ions, as we have reported the synthesis of the zigzag-chain, cyclic-octanuclear Ca(II) and hexanuclear Na(I) complexes, using bulky amide ligands, benzoylamino groups.[24] Here, we have succeeded in the isolation and characterization of the first example of mononuclear Ca(II) complexes with a phosphate monoanion and dianion using such extremely bulky amide ligands as models of the mononuclear Ca(II) core contained in the phosphotransferase active site. In this paper, we will discuss the formation of NH···O hydrogen bonds between amide NHs and the oxygen atoms of phosphate among the three states, that is, the acid, the monoanion, and the dianion, and the properties of the Ca−O(phosphate) bonds on the basis of the X-ray analysis and IR and ^{1}H NMR spectroscopy.

Experimental Section

Materials. All solvents were distilled over appropriate drying agents and degassed prior to use. All starting reagents were of commercial grade. 2,6-$(Ph_3CCONH)_2C_6H_3OPO_3H_2$ (**1**) was synthesized by literature methods.[25] 2,6-$^i Pr_2C_6H_3OPO_3H_2$ was synthesized by literature methods.[26]

2,6-$(Ph_3CCONH)_2C_6H_3OH$. A mixture of 4.3 g (14 mmol) of CPh_3COCl and 1.27 g (6.5 mmol) of 2,6-$(NH_2)C_6H_3OH\cdot 2HCl$ was suspended in 70 mL of dichloromethane. A 3.9 mL (28 mmol) portion of NEt_3 was added dropwise to the suspension. After being stirred for 4 h, the mixture was diluted with 400 mL of dichloromethane and washed with aq HCl, followed by washing with aq 5% $NaHCO_3$ and NaCl saturated solutions. The organic layer separated was concentrated under reduced pressure to give a white precipitate. Yield, 90%. Anal. Calcd for $C_{46}H_{36}N_2O_3$: C, 83.11; H, 5.46; N, 4.21. Found: C, 82.67; H, 5.40; N, 4.47.

2,6-$(Ph_3CCONH)_2C_6H_3OPO_3H_2$ (1). To a solution of 1.0 mL (11 mmol) of $POCl_3$ and 1.7 mL (21 mmol) of pyridine in 3 mL of dichloromethane was added a solution of 2,6-bis(triphenylacetylamino)phenol (1.6 g, 2.4 mmol) in 40 mL of dichloromethane with vigorous stirring at 0 C°. After 2 h, aqueous acetone was added and refluxed until hydrolysis was finished. The solution was concentrated in vacuo, and the residue was extracted with dichloromethane. The solution was washed with 1 M aq HCl to remove pyridine. The organic layer was evaporated, and the crude material was recrystallized from hot methanol to give colorless crystals. Yield, 32%. ^{1}H NMR (DMSO-d_6): δ 8.96 (s, 2H, NH), 7.88 (d (J = 8.2 Hz), 2H, m-ArH), 8.29−7.21 (m, 32H, PhH and *m*-ArH), 6.72 (t (J = 8.2 Hz), 1H, *p*-ArH). ^{31}P NMR (DMSO-d_6): δ −1.13 ppm. ^{31}P NMR (in the solid state): δ −1.2 ppm. Anal. Calcd for $C_{51}H_{40}N_3O_5P_1\cdot(H_2O)$: C, 72.43; H, 5.15; N, 3.67. Found: C, 72.08; H, 5.14; N, 3.71.

(C_5H_5NH)\{2,6-$(Ph_3CCONH)_2C_6H_3OPO_3H$\} (2a). To a solution of 0.12 mL (1.4 mmol) of $POCl_3$ and 0.21 mL (2.8 mmol) of pyridine in 0.4 mL of dichloromethane was added a solution of 2,6-bis(triphenylacetylamino)phenol in 2 mL of dichloromethane with stirring at 0 C°. After 2 h, aqueous acetone was added and the mixture refluxed until hydrolysis was finished. The solution was concentrated to give a pale yellow powder. Recrystallization from ethyl acetate followed by acetonitrile gave colorless crystals. Yield, 30%. Anal. Calcd for $C_{51}H_{42}N_3O_6P_1$: C, 74.35; H, 5.14; N, 5.10. Found: C, 74.29; H, 5.06; N, 5.26.

(NEt_4)\{2,6-$(Ph_3CCONH)_2C_6H_3OPO_3H$\} (2b). Compound **1** (76.5 mg, 0.10 mmol) and $(NEt_4)(OAc)\cdot H_2O$ (26 mg, 0.10 mmol) were dissolved in THF/ethanol solution and concentrated to dryness. The residue was recrystallized from acetonitrile/THF to give colorless crystals. Yield, 52%. ^{1}H NMR (DMSO-d_6): δ 9.96 (s, 2H, NH), 7.43 (d (J = 8.3 Hz), 2H, *m*-ArH), 7.29−7.15 (m, 30H, PhH), 6.88 (t (J = 8.3 Hz), 1H, *p*-ArH). Anal. Calcd for $C_{51}H_{42}N_3O_6P_1\cdot(H_2O)_3$: C, 69.89; H, 6.73; N, 4.53. Found: C, 70.10; H, 6.95; N, 4.31.

(10) Albert, J. S.; Goodman, M. S.; Hamilton, A. D. *J. Am. Chem. Soc.* **1995**, *117*, 1143−1144.
(11) Iverson, B. L.; Shreder, K.; Kra'l, V.; Sansom, P.; Lynch, V.; Sessler, J. L. *J. Am. Chem. Soc.* **1996**, *118*, 1608−1616.
(12) Jubian, V.; Dixon, R. P.; Hamilton, A. D. *J. Am. Chem. Soc.* **1992**, *114*, 1120−1121.
(13) Breslow, R.; Bovy, P.; Hersh, A. L. *J. Am. Chem. Soc.* **1980**, *102*, 2115−2116.
(14) Kràl, V.; Furuta, H.; Shreder, K.; Lynch, V.; Sessler, J. L. *J. Am. Chem. Soc.* **1996**, *118*, 1595−1607.
(15) Schmidtchen, F. P.; Berger, M. *Chem. Rev.* **1997**, *97*, 1609−1646.
(16) Li, C.-T.; Caughlan, C. N. *Acta Crystallogr.* **1965**, *19*, 637−645.
(17) Bissinger, P.; Kumberger, O.; Schier, A. *Chem. Ber.* **1990**, *124*, 509−513.
(18) Sato, T. *Acta Crystallogr.* **1984**, *C40*, 738−740.
(19) Sato, T. *Acta Crystallogr.* **1984**, *C40*, 736−738.
(20) Cao, G.; Lee, H.; Lynch, V. M.; Mallouk, T. E. *Inorg. Chem.* **1988**, *27*, 2781−2785.
(21) Cao, G.; Lynch, V. M.; Swinnea, S.; Mallouk, T. E. *Inorg. Chem.* **1990**, *29*, 2112−2117.
(22) Uchtmann, V. A. *J. Phys. Chem.* **1972**, *76*, 1304−14310.
(23) Rudolf, P. R.; Clarke, E. T.; Martell, A. E.; Clearfield, A. *Acta Crystallogr.* **1988**, *C44*, 796−799.
(24) Onoda, A.; Yamada, Y.; Okamura, T.; Doi, M.; Yamamoto, H.; Ueyama, N. *J. Am. Chem. Soc.* **2002**, *124*, 1052.
(25) Sowa, T.; Ouchi, S. *Bull. Chem. Soc. Jpn.* **1975**, *48*, 2084.
(26) Kosolapoff, G. M.; Arpke, C. K.; Lamb, R. W.; Reich, H. *J. Chem. Soc. C* **1968**, 815−818.

Table 1. Crystallographic Data for **1**, **2a**, **3**, and **4**

	1·$(MeOH)_2$	**2a**	**3**·$(H_2O)_7(CH_3CN)_9$	**4**
empirical formula	$C_{48}H_{45}N_2O_8P$	$C_{51}H_{42}N_3O_6P$	$C_{166}H_{170}CaN_{19}O_{25}P_3$	$C_{48}H_{49}CaN_2O_{11}P$
fw	808.87	823.85	2964.2	900.94
color	colorless	colorless	colorless	colorless
cryst syst	triclinic	orthorhombic	trigonal	orthorhombic
space group	$P\bar{1}$ (No. 2)	*Pbcn* (No. 60)	$P\bar{3}$ (No. 147)	*Pnma* (No. 62)
a, Å	14.780(2)	15.009(5)	19.128(4)	9.8219(8)
b, Å	16.392(3)	17.797(4)	19.128(4)	32.729(2)
c,Å	8.873(2)	31.461(5)	27.937(7)	14.2572(11)
α, deg	90.43(2)	90	90	90
β, deg	104.50(2)	90	90	90
γ, deg	94.92(1)	90	120	90
V, Å^3	2072.6(7)	8404(3)	8852(3)	4583.2(6)
Z	2	8	2	4
ρ_{calcd}, g cm^{-1}	1.296	1.302	1.112	1.306
μ (Mo Kα), cm^{-1}	1.24	1.22	1.29	2.34
temp (K)	296	296	296	296
scan type	$\omega-2\theta$	$\omega-2\theta$	$\omega-2\theta$	ω
$2\theta_{max}$, deg	55.0	50.0	55.0	55.0
no. collected reflns	10151	8133	14441	18616
no. unique reflns	9535	7403	13562	5213
no. reflns used	7141 ($I > 3\sigma(I)$)	7403 (all data)	13562 (all data)	5213 (all data)
no. variables	532	551	635	296
GOF	1.859	0.888	0.947	0.913
R1[a]	0.043 (R^c)	0.042	0.067	0.114
wR2[b]	0.065 ($R_w{}^d$)	0.141	0.249	0.348

[a] $R1 = \sum||F_o| - |F_c||/\sum|F_o|$. [$I > 2\sigma(I)$]. [b] $wR2 = [\sum w(F_o^2 - F_c^2)^2/\sum w(F_o^2)^2]^{1/2}$. [c] $R = \sum||F_o| - |F_c||/\sum|F_o|$. [d] $R_w = [\sum w(|F_o| - |F_c|)^2/\sum w|F_o|^2]^{1/2}$; $w = 1/\sigma^2(|F_o|)$.

$(NMe_4)[Ca^{II}\{O_2P(OH)OC_6H_3$-2,6-$(NHCOCPh_3)_2\}_3(N{\equiv}C$-$Me)_3]$ (3). To a solution of 118 g (0.15 mmol) of 2,6-$(Ph_3$-$CCONH)_2C_6H_3OPO_3H_2$·H_2O in THF/EtOH was added a solution of 9.1 mg (0.05 mmol) of $Ca(OAc)_2$·H_2O and 6.8 mg (0.05 mmol) of $(NMe_4)(OAc)$ in EtOH/H_2O. The solution was concentrated in vacuo, and the residue was recrystallized from hot acetonitrile to give colorless hexagonal crystals. Yield, 42%. Anal. Calcd for $C_{142}H_{120}CaN_7O_{18}P_3$·$(H_2O)_5(MeCN)_2$: C, 69.65; H, 5.44; N, 5.01. Found: C, 69.76; H, 5.40; N, 4.86.

$[Ca^{II}\{O_3POC_6H_3$-2,6-$(NHCOCPh_3)_2\}(H_2O)_3(MeOH)_2]$ (4). To a solution of 81 mg (0.11 mmol) of 2,6-$(Ph_3CCONH)_2C_6H_3$-OPO_3H_2·H_2O in THF/EtOH was added a solution of 18.7 mg (0.11 mmol) of $Ca(OAc)_2$·H_2O in EtOH/H_2O. The solution was concentrated in vacuo, and the residue was recrystallized from hot MeOH to give colorless crystals. Yield, 40%. Anal. Calcd for $C_{142}H_{120}$-$CaN_7O_{18}P_3$·$(H_2O)_2$·$(MeOH)_3$: C, 64.32; H, 5.62; N, 3.06. Found: C, 65.66; H, 6.09; N, 2.70.

$(NEt_4)[Ca^{II}\{O_2P(OH)OC_6H_3$-2,6-$^i Pr_2\}_3(H_2O)_3]$. A 39.5 mg (0.15 mmol) portion of 2,6-$^i Pr_2C_6H_3OPO_3H_2$, 9.0 mg (0.05 mmol) of $Ca(OAc)_2$·H_2O, and 13.3 mg (0.05 mmol) of $(NEt_4)(OAc)$ were dissolved in methanol. The solution was warmed and concentrated several times to give colorless crystals. Yield, 85%. Anal. Calcd for $C_{44}H_{80}CaNO_{15}P_3$: C, 53.05; H, 8.09; N, 1.41. Found: C, 53.05; H, 8.10; N, 1.45.

Physical Measurement. ^{1}H NMR and ^{31}P NMR spectra in solution were recorded on a JEOL EX 270 or a JEOL EX 400 spectrometer. ^{31}P NMR spectra in the solid state were recorded on a Chemmagnetics CMX-300. IR spectra in the solid state of KBr pellets were taken on a Jasco FT/IR-8300 spectrometer. pK_a measurement was performed on a Metrohm 716 DMS Titrino. The pK_a value for **1** was measured in 50% THF/aqueous solution. Triton X-100 micelles were used.

X-ray Structure Determination. Single crystals of 2,6-$(Ph_3$-$CCONH)_2C_6H_3OPO_3H_2$ (**1**), $(C_5H_5NH)\{2,6$-$(Ph_3CCONH)_2C_6H_3$-$OPO_3H\}$ (**2a**), $(NMe_4)[Ca^{II}\{O_2P(OH)OC_6H_3$-2,6-$(NHCOCPh_3)_2\}_3$-$(N{\equiv}CMe)_3]$ (**3**), and $[Ca^{II}\{O_3POC_6H_3$-2,6-$(NHCOCPh_3)_2\}(H_2O)_3$-$(MeOH)_2]$ (**4**) were sealed in glass capillaries. The X-ray data for **1**, **2a**, and **3** were collected at 296 K on a Rigaku AFC5R or an AFC7R diffractometer equipped with a rotating anode X-ray generator. The radiation used was Mo Kα monochromatized with graphite (0.71069 Å). No empirical absorption correction was applied. Unit cell dimensions were refined by 20 reflections. These standard reflections were monitored with every 150 reflections and did not show any significant change. The X-ray data for **4** were collected in 2.0° oscillation at 296 K on a Raxis RAPID. A sweep of data for **4** was done using ω oscillations from 130.0° to 190.0° at $\phi = 0.0°$ and $\chi = 45.0°$, and from 0.0° to 160.0° at $\phi = 180.0°$ and $\chi = 45.0°$. The basic crystallographic parameters for **1**, **2a**, **3**, and **4** are listed in Table 1. The structures were solved by the direct method and expanded using Fourier techniques using a *teXsan* crystallographic software [27] and *SHELXL-97*.[28] Non-hydrogen atoms except for the solvent water molecules for **3** were refined anisotropically, and the hydrogen atoms were refined isotropically.

Density Functional Calculations. DFT calculations using Becke's three-parameter hybrid functional with the coorelation functional of Lee, Yang, and Parr (B3LYP)[29−31] were performed using the program package Gaussian 98.[32] Single point calculations for models **6** and **7**, which are built on the basis of the crystal structure, were carried out with 6311+g(d,p) basis set for Ca, 631+g(d,p) basis set for O, N and 6−31 g basis set for P, C, H atoms.

Results

Crystal Structures of the Phosphate Ligands. Crystal structure analyses show hydrogen bonding interactions

(27) *teXsan: Crystal Structure Analysis Package*; Molecular Structure Corporation: The Woodland, TX, 1985, 1999.
(28) Sheldrick, G. M. *SHELXL-97, Program for the Refinement of Crystal Structures*; University of Göttingen: Göttingen, Germany, 1997.
(29) Becke, A. D. *Phys. Rev. A* **1988**, *38*, 3098−3100.
(30) Lee, C.; Yang, W.; Parr, R. G. *Phys. Rev. B* **1988**, *37*, 7685−7789.
(31) Becke, A. D. *J. Chem. Phys.* **1993**, *98*, 5648−5652.

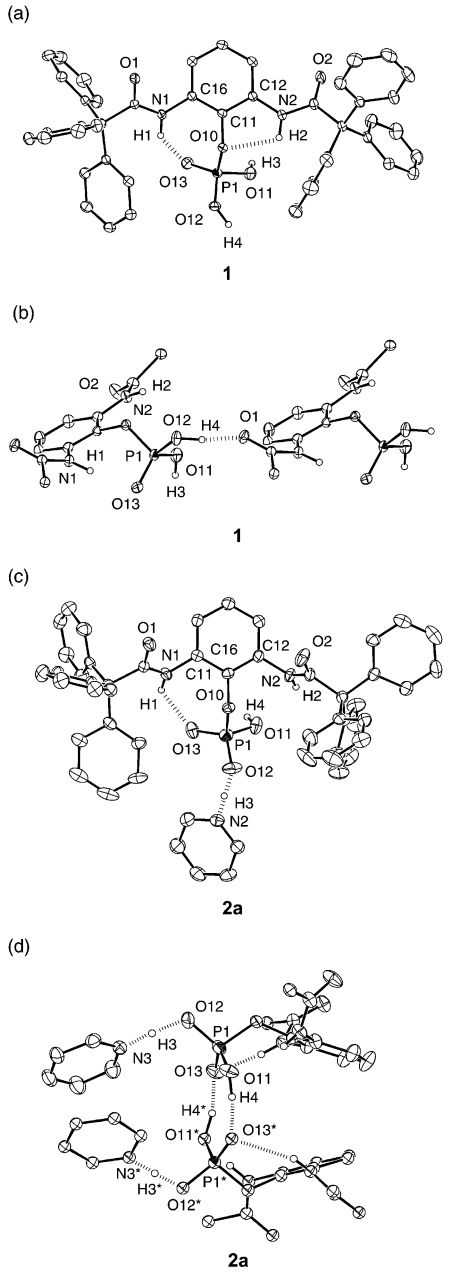

Figure 2. Molecular and dimeric structure of (a) 2,6-$(Ph_3CCONH)_2C_6H_3OPO_3H_2$ (**1**), (b) intermolecular hydrogen bond for **1**, (c) (C_5H_5NH)\{2,6-$(Ph_3CCONH)_2C_6H_3OPO_3H$\} (**2a**), and (d) intermolecular hydrogen bond of **2a** in the solid state The dashed lines indicate the hydrogen bonds. The CPh_3 groups are omitted for clarity in the dimeric representation.

between amide groups and phosphate groups. Figure 2a,b shows the crystal structure of the phosphate ligand in the phosphoric acid state, 2,6-$(Ph_3CCONH)_2C_6H_3OPO_3H_2$ (**1**),

Table 2. Selected Bond Distances (Å), Bond Angles (deg), and Torsion Angles (deg) for **1**

P(1)−O(10)	1.608(1)	P(1)−O(11)	1.533(1)
P(1)−O(12)	1.540(1)	P(1)−O(13)	1.468(1)
N(1)···O(10)	2.782(1)	H(1)···O(10)	2.579
N(2)···O(10)	2.780(1)	H(2)···O(10)	2.293
N(1)···O(13)	2.860(2)	H(1)···O(13)	2.071
N(2)···O(11)	3.294(2)	H(2)···O(11)	2.872
O(1)−O(12)	2.632(1)	H(4)−O(1)	1.641

O(10)−P(1)−O(11)	106.54(7)	O(10)−P(1)−O(12)	99.50(7)
O(10)−P(1)−O13)	109.78(7)	O(11)−P(1)−O(12)	107.36(8)
O(11)−P(1)−O(13)	116.21(9)	O(12)−P(1)−O(13)	115.81(8)
N(1)−H(1)−O(13)	139.58	N(2)−H(2)−O(11)	108.12
C(11)−C(12)−N(2)−C(18)	174.2(2)	C(11)−C(16)−N(1)−C(17)	142.8(2)

Table 3. Selected Bond Distances (Å), Bond Angles (deg), and Torsion Angles (deg) for **2a**

P(1)−O(10)	1.617(3)	P(1)−O(11)	1.553(3)
P(1)−O(12)	1.488(3)	P(1)−O(13)	1.506(3)
N(1)···O(10)	2.795(4)	H(1)···O(10)	2.825
N(2)···O(10)	2.758(4)	H(2)···O(10)	2.980
N(1)···O(13)	2.983(5)	H(1)···O(13)	2.309
N(2)···O(11)	2.949(5)	H(12)···O(11)	2.422
N(3)···O(12)	2.567(5)	H(3)···O(12)	1.334
N(3)···H(3)	1.236		
O(11)···O(13)	2.491(4)	H(4)···O(13)	1.522

O(10)−P(1)−O(11)	104.4(2)	O(10)−P(1)−O(12)	102.7(2)
O(10)−P(1)−O13)	107.4(2)	O(11)−P(1)−O(12)	112.5(2)
O(11)−P(1)−O(13)	111.1(2)	O(12)−P(1)−O(13)	117.4(2)
N(1)−H(1)···O(11)	135.4	N(2)−H(2)···O(12)	120.2
C(17)−N(1)−C(12)−C(11)	123.1(5)	C(19)−N(2)−C(16)−C(11)	−104.0(5)

and the linkage of the units via intermolecular P−OH···O═C hydrogen bonds (Figure 2b). The selected bond distances and angles are listed in Table 2. The distances of amide N and phosphate O atoms, N1···O13 (2.860(2) Å) and H1···O13 (2.071 Å), indicate the presence of a hydrogen bond. The phenyl plane of the aryl phosphate compounds usually lies in parallel to the P−O−C(Ar) plane, but these planes in **1** are nearly perpendicular (98.25°) to each other because of the presence of the NH···O(−P) hydrogen bonds. The amide NH2 proton directs to the O12 atom on the basis of the N2···O10 (2.780(1) Å) and H2···O10 (2.293 Å) distances. The bond distances of P1−O11, P1−O12, and P1−O13 are 1.533(1), 1.540(1), and 1.468(1) Å, respectively. The oxygen atoms of O11 and O12 are identified to be a part of a P−OH single bond, and P1−O13 is ascribed to a P═O double bond compared with the reported bond distances.[33] Therefore, the amide NH1 proton directs to an oxygen atom of the P═O double bond, while the amide NH2 proton does not to the opposite side of the oxygen atom of the P−O−H single bond but to that of the P−O−C bond.

These hydrogen bonding interactions between amide groups and phosphate groups are different depending on the anionic state of the phosphate part. The molecular structure of the phosphate ligand in the monoanion state, (C_5H_5NH)-\{2,6-$(Ph_3CCONH)_2C_6H_3OPO_3H$\} (**2a**), is shown in Figure 2c, and the selected bond distances and angles of **2a** are listed in Table 3. The P−O distances for **2a** indicate that one oxygen atom is protonated to give P−OH, and the anionic charge is delocalized over the other two P−O bonds. The distances of N1···O13 (2.983(5) Å) and H1···O13 (2.309

(32) Frisch, M. J.; Trucks, G. W.; Schlegel, H. B.; Scuseria, G. E.; Robb, M. A.; Cheeseman, J. R.; Zakrzewski, V. G.; Montgomery, J. A., Jr.; Stratmann, R. E.; Burant, J. C.; Dapprich, S.; Millam, J. M.; Daniels, A. D.; Kudin, K. N.; Strain, M. C.; Farkas, O.; Tomasi, J.; Barone, V.; Cossi, M.; Cammi, R.; Mennucci, B.; Pomelli, C.; Adamo, C.; Clifford, S.; Ochterski, J.; Petersson, G. A.; Ayala, P. Y.; Cui, Q.; Morokuma, K.; Malick, D. K.; Rabuck, A. D.; Raghavachari, K.; Foresman, J. B.; Cioslowski, J.; Ortiz, J. V.; Stefanov, B. B.; Liu, G.; Liashenko, A.; Piskorz, P.; Komaromi, I.; Gomperts, R.; Martin, R. L.; Fox, D. J.; Keith, T.; Al-Laham, M. A.; Peng, C. Y.; Nanayakkara, A.; Gonzalez, C.; Challacombe, M.; Gill, P. M. W.; Johnson, B. G.; Chen, W.; Wong, M. W.; Andres, J. L.; Head-Gordon, M.; Replogle, E. S.; Pople, J. A. *Gaussian 98*, revision A.1; Gaussian, Inc.: Pittsburgh, PA, 1998.

(33) Schneider, B.; Kabelac, M.; Hobza, P. *J. Am. Chem. Soc.* **1996**, *118*, 8, 12207−12217.

Å) indicate that the amide NH1 proton directs to the O13 atom having an anionic charge. O12 is also involved in hydrogen bonding with N2 of pyridine because of the short N3···O12 distance (2.576(6) Å). The other amide NH2 proton does not direct to both O10 from P−O−C and O11 from P−O−H and is free from hydrogen bond interaction. The P−OH oxygen atom is in the range for the formation of the P−OH···O−P hydrogen bonds with the neighboring molecule for **2a** as shown in Figure 2d. The dimer unit structures with P−OH···O−P hydrogen bonds were observed in the phosphate monoanion state.

Crystal Structures of Ca(II) Complexes. We have isolated a novel homoleptic Ca(II)−phosphate complex with a mononuclear core using bulky triphenylacylamino ligands. Figure 3a shows the molecular structure of the Ca(II) complex with the phosphate monoanion ligand, $(NMe_4)[Ca^{II}\{O_2P(OH)OC_6H_3\text{-}2,6\text{-}(NHCOCPh_3)_2\}_3(N{\equiv}CMe)_3]$ (**3**), and the selected bond distances and angles of **3** are listed in Table 4. Compound **3** has a mononuclear Ca(II) core having a distorted octahedral geometry with crystallographic C_3 symmetry. The Ca(II) ion is ligated with each of the oxygen atoms (O11) of the three phosphate monoanion ligands and the nitrogen atoms from three acetonitrile molecules in a *facial* mode (Figure 3b,c). The short distance between the two uncoordinated oxygen atoms, O12 and O13* (2.544(4) Å), indicates the formation of P−OH···O=P hydrogen bonds forming a 13-membered ring among the three phosphate monoanion ligands which can produce the *facial* coordination. The P−OH···OH hydrogen bonds normally form infinite networks, such as 1D or 2D.[16,21] Such a hydrogen bonding network can be interrupted by the bulkiness of the ligand and the hydrogen bonding from the amide NH to the P−O oxygen atom, as shown in Figure 3b. These intramolecular interactions cause the present cylic P−OH···OH hydrogen bond, which can induce the mononuclear Ca(II) core.

In this mononuclear complex, the phosphate oxygen atoms coordinate within short distances. The Ca1−O11 bond distance of **3** is 2.262(4) Å, which is in the range of the shortest Ca−O(phosphate) bond. The O11 atom coordinates in *syn* type with an angle of 142.2(2)° (Ca1−O11−P1). The bond distances of P1−O11, P1−O12, and P1−O13 are 1.480(4), 1.494(4), and 1.539(4) Å, respectively. The P−O bond distances indicate that P1−O11 and P1−O12 form a conjugated anion. The Ca1−N3 distance (2.517(7) Å) and the Ca1−N3−C81 angle (168.1(7)°) are in the range of the reported Ca(II)−acetonitrile complexes (2.43−2.54 Å, 151.0−177.4°).[34−36]

Our bulky triphenylacylamino ligand can also form a mononuclear Ca(II) core in the phosphate dianion state. Figure 4a shows the molecular structure of a Ca(II) complex, $[Ca^{II}\{O_3POC_6H_3\text{-}2,6\text{-}(NHCOCPh_3)_2\}(H_2O)_3(MeOH)_2]$ (**4**), with the phosphate dianion ligand, and the selected bond lengths and bond angles for **4** are listed in Table 5. The Ca(II) center is in an octahedral geometry with oxygen atoms of the phosphate ligand, three water molecules, and two methanol molecules. Compound **4** has crystallographic symmetry over the Ca1−O11−P1 plane. The dianion ligand coordinates in a monodentate fashion. The Ca1−O11 dis-

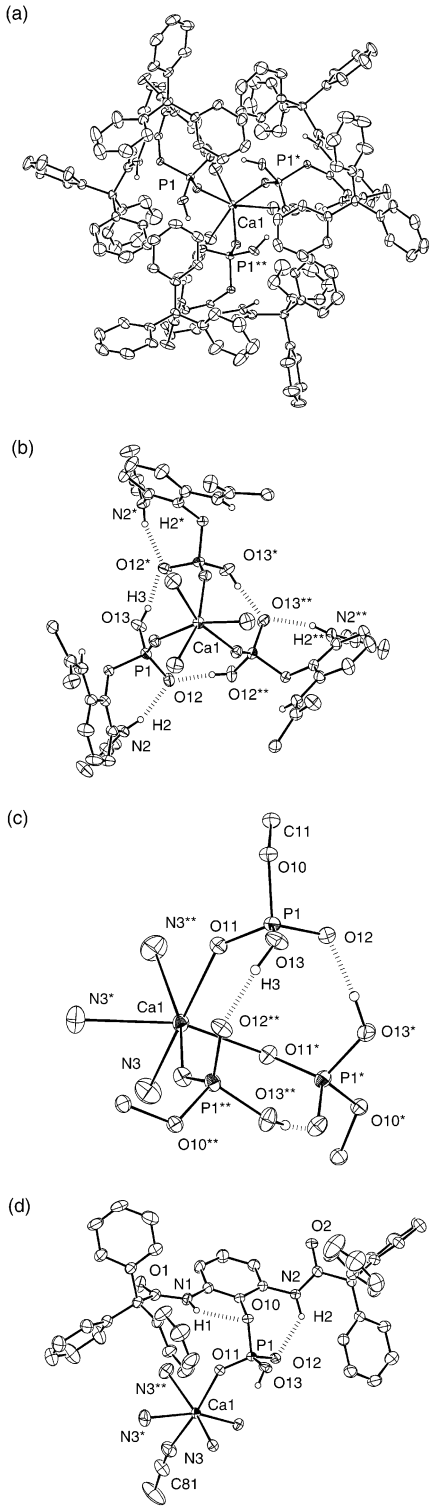

Figure 3. (a) Anion part structure, (b) zoomed Ca(II) core structure, (c) Ca(II) coordination sphere, and (d) symmetric unit structure of $(NMe_4)[Ca^{II}\{O_2P(OH)OC_6H_3\text{-}2,6\text{-}(NHCOCPh_3)_2\}_3(N{\equiv}CMe)_3]$ (**3**). The solute molecules involved are omitted for clarity. The dotted line refers to a hydrogen bond involving a proton.

(34) Khattar, R.; Knobler, C. B.; Hawthorne, M. F. *J. Am. Chem. Soc.* **1996**, *112*, 4962−4963.
(35) Waters, A. F.; White, A. H. *Aust. J. Chem.* **1996**, *49*, 27−34.
(36) Raevskii, O. A.; Tkachev, V. V.; Atovmyan, L. O.; Zuvareba, V. E.; Bulgak, I. I.; Batyr, D. G. *Koord. Khim.* **1988**, *14*, 1697−1704.

Table 4. Selected Bond Distances (Å), Bond Angles (deg), and Torsion Angles (deg) for **3**

Ca(1)−O(11)	2.262(4)	Ca(1)−N(3)	2.519(6)
P(1)−O(10)	1.634(3)	P(1)−O(11)	1.480(4)
P(1)−O(12)	1.494(4)	P(1)−O(13)	1.539(4)
N(1)···O(10)	2.683(6)	H(1)···O(10)	2.295
N(2)···O(10)	2.799(5)	H(2)···O(10)	2.779
N(1)···O(11)	3.329(7)	H(1)···O(11)	2.986
N(2)···O(12)	2.827(6)	H(2)···O(12)	2.155
O(12)···O(13)	2.544(4)	H(3)···O(12)	2.985
Ca(1)−O(11)−P(1)	142.2(2)	Ca(1)−N(3)−C(81)	168.2(7)
O(10)−P(1)−O(11)	109.1(2)	O(10)−P(1)−O(12)	105.7(2)
O(10)−P(1)−O13)	98.5(2)	O(11)−P(1)−O(12)	116.2(2)
O(11)−P(1)−O(13)	113.5(2)	O(12)−P(1)−O(13)	112.0(2)
N(1)−H(1)···O(11)	106.1	N(2)−H(2)···O(12)	134.7
C(17)−N(1)−C(12)−C(11)	−172.8(6)	C(19)−N(2)−C(16)−C(11)	−124.3(6)

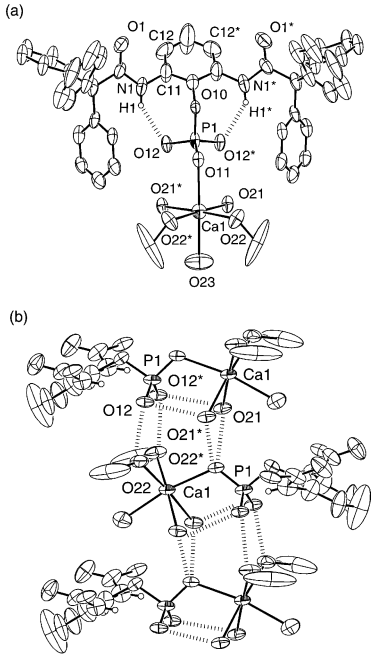

Figure 4. (a) Molecular structure and (b) packing structure of $[Ca^{II}\{O_3POC_6H_3\text{-}2,6\text{-}(NHCOCPh_3)_2\}(H_2O)_3(MeOH)_2]$ (**4**).

Table 5. Selected Bond Distances (Å), Bond Angles (deg), and Torsion Angles (deg) for **4**

Ca(1)−O(11)	2.392(8)	Ca(1)−O(21)	2.372(5)
Ca(1)−O(22)	2.285(6)	Ca(1)−O(23)	2.394(13)
P(1)−O(10)	1.634(7)	P(1)−O(11)	1.536(7)
P(1)−O(12)	1.504(4)		
N(1)···O(10)	2.790	H(1)···O(10)	2.642
N(1)···O(12)	2.94(1)	H(1)···O(12)	2.243
O(12)···O(21)	2.848(8)	O(12)···O(22)	2.575(6)
Ca(1)−O(11)−P(1)	117.9(3)	O(10)−P(1)−O(11)	102.7(4)
O(10)−P(1)−O(12)	106.3(3)	O(11)−P(1)−O(12)	112.8(3)
O(12)−P(1)−O(12)	114.7(4)	N(1)−H(1)···O(11)	138.2
C(11)−C(12)−N(1)−C(15)	135.2(12)		

tance is 2.392(8) Å, and O11 coordinates in a *syn* type with angles of 117.9(3)°. This mononuclear unit is stacked with intermolecular OH···O hydrogen bonds between O11 and O12, O12 and O22, as shown in Figure 4b.

The hydrogen bond interaction with the amide NHs is different between the charged states (monoanion/dianion) of the coordinating phosphate group. In the phosphate monoanion complex, **3**, only one amide NH is hydrogen-bonded with the P−O oxygen (N2···O12 (2.827(6) Å), H2···O12 (2.155 Å)). The other one, NH1 proton, is directed to the O10 atom (N1···O10 (2.683(6) Å), H1···O10 (2.295 Å)), while both amide NHs are intramolecularly hydrogen-bonded in the phosphate dianion complex, **4**. The bond distances of N1···O12 and H1···O12 are 2.94(1) and 2.151 Å. Therefore, the NH···O hydrogen bonds with the phosphate groups tend to be formed more preferentially in the dianion state than in the monoanion state.

Table 6. Selected IR Bands for Various Phosphate Ligands and Ca(II) Complexes in the Solid State (KBr)

	IR bands (cm^{-1})		
	ν(OH)	ν(NH)	ν(C═O)
1	3440 (br)	3431	1684
2b	3440 (br)	3404	1676
3	3440 (br)	3389	1669
4	3430 (br)	3254	1656

IR Spectra in the Solid State. The formation of hydrogen bonds for **1**, **2b**, **3**, and **4** in the solid state was determined by IR spectroscopy. The selected IR bands of the ν(OH), ν(NH), and ν(C═O) region for **1**, **2b**, **3**, and **4** are listed in Table 6. The downshifted broad OH bands around 3400 cm^{-1} are due to the formation of hydrogen bonds with C═O or P—O oxygen in the solid state. Actually, the crystal structure analysis indicates intermolecular P—OH···O═C hydrogen bonds or P—OH···O—P hydrogen bonds for the phosphate monoanion ligands. The OH bands for **4** are originated from the water molecules coordinating to Ca(II) ions. The free amide NH bands are known to appear in the range 3400−3500 cm^{-1}.[37] Thus, the amide NH band of **1**, **2b**, and **3** around 3400 cm^{-1} indicates the absence of the NH···O hydrogen bonds. The largely shifted (∼200 cm^{-1}) NH band for **4** at 3254 cm^{-1} reveals the formation of strong NH···O hydrogen bonds in the phosphate dianion state.

^{1}H NMR Spectra. The strength of NH···O hydrogen bonds in the solution state was estimated by ^{1}H NMR spectroscopy. The amide NH chemical shifts for **1**, **2b** and **3** in 5 mM DMSO-d_6 are 8.9, 10.0, and 9.9 ppm, respectively. The NH signals of **2b** and **3** are downfield shifted by 1.1 and 1.0 ppm from that of **1** in the phosphoric acid state, respectively. Generally, amide NH signals are known to shift by the strong solvation of DMSO to the amide plane. However, similar NH chemical shifts for **1** (8.9 ppm in THF-d_8 solution) and for **2b** (10.0 ppm in acetonitrile-d_3) in less

(37) Silverstein, R. M.; Bassler, G. C.; Morrill, T. C. *Spectrometric Identification of Organic Compounds*; Wiley: New York, 1981.

Scheme 2. Ligand Exchange Reactions with the Phosphate Ligand with the Amide Groups

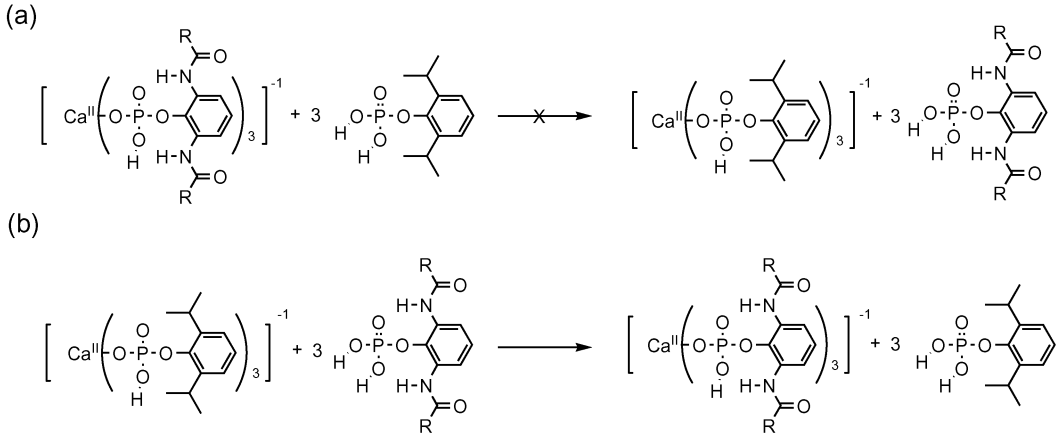

polar solvent indicate that the amide NH protons are free from solvation of DMSO because of the bulky CPh_3 groups. The amide NH chemical shifts indicate that the NH···O hydrogen bond between the amide NH and the oxygen atom of phosphate is absent in the phosphoric acid state but is formed in the phosphate monoanion state.

Ligand-Exchange Reaction in Mononuclear Ca(II)−Phosphate Complex. The ligand-exchange reaction of the hydrogen-bonded mononuclear Ca(II) phosphate complex, **3**, was examined using ^{1}H NMR spectroscopy. Mononuclear structure is extensively important for the purpose of detailed discussion about the effect of NH···O hydrogen bonds on the Ca−O bond dissociation. As already mentioned, the amide NH chemical shifts in the phosphoric acid state and in the monoanion state were 8.96 and 9.92 ppm, respectively. Thus, the NH chemical shifts of the amide group can be utilized as a probe for investigation of the electronic state of the phosphate ligand. Figure 5 shows the ^{1}H NMR spectra of the ligand-exchange reaction of **3** with the addition of 3 and 12 equimolar amounts of 2,6-^{i}Pr$_2$C$_6$H$_3$OPO$_3$H$_2$. The amide NH signals in mixed solution indicate that the phosphate anion in **3** is not protonated with the addition of the excess 2,6-^{i}Pr$_2$C$_6$H$_3$OPO$_3$H$_2$ and the ligand-exchange reaction does not proceed as shown in Scheme 2a. Therefore, the NH···O hydrogen-bonded phosphate ligands coordinate to Ca(II) ion as phosphate monoanions and prevent the coordination of the ^{i}Pr-substituted phosphate ligands.

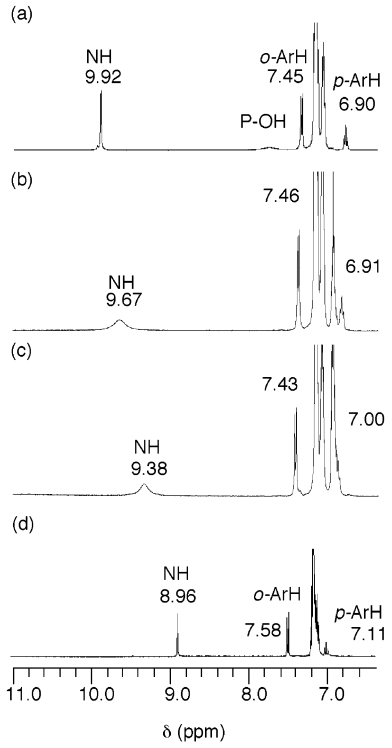

Figure 5. Ligand exchange reaction of (NMe$_4$)[Ca^{II}{O$_2$P(OH)OC$_6$H$_3$-2,6-(NHCOCPh$_3$)$_2$}$_3$(N≡CMe)$_3$] (**3**) with 2,6-^{i}Pr$_2$C$_6$H$_3$OPO$_3$H$_2$ examined by ^{1}H NMR spectra in Me$_2$SO-d_6 at 30 °C. The spectra of (a) **3**, (b) **3** with 3 equiv (1 equiv to ligands), (c) **3** with 12 equiv (4 equiv to ligands), and (d) **1** are shown.

The reverse ligand-exchange reaction as shown in Scheme 2b was performed under the same conditions. The Ca(II)−phosphate complex without hydrogen bonds, (NEt$_4$)[Ca^{II}-{O$_2$P(OH)OC$_6$H$_3$-2,6-^{i}Pr$_2$}$_3$(H$_2$O)$_3$], was added with 3-fold excess of hydrogen-bonded ligand, **1**. The amide NH signal at 8.96 ppm for **1** shifted downfield to 9.97 ppm, as shown in Figure 6. Thus, the phosphoric acid ligand, **1**, immediately coordinates to a Ca(II) ion as a monoanion ligand. The two pK_a values (pK_{a1}, pK_{a2}) for **1** and 2,6-^{i}Pr$_2$C$_6$H$_3$OPO$_3$H$_2$ are 3.3, 7.9 and 3.6, 8.0 in 50% aqueous THF solution. Consequently, the NH···O hydrogen bonds to the phosphate ligand lowered the pK_a value of phosphate groups and enforced the formation of the Ca−O bonds.

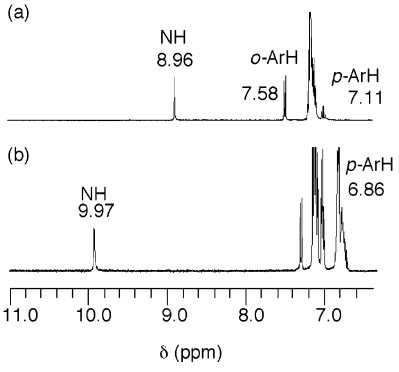

Figure 6. Ligand exchange reaction of (NEt$_4$)[Ca^{II}{O$_2$P(OH)OC$_6$H$_3$-2,6-iPr$_2$}$_3$] with 2,6-(Ph$_3$CCONH)$_2$C$_6$H$_3$OPO$_3$H$_2$ examined by ^{1}H NMR spectra, which are shown for (a) **1** and (b) **3** with $^1/_3$ equiv (1 equiv to ligands).

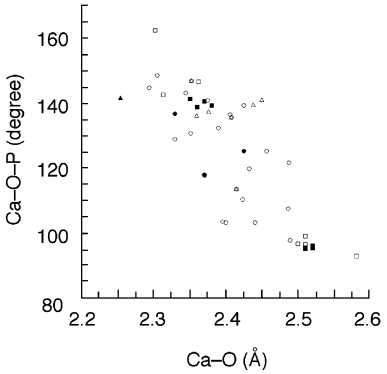

Figure 7. Scatter plot of Ca−O bond distances and Ca−O−P bond angles among various $Ca(O_3POR)$ and $Ca(O_3PR)$ complexes.[16−23,38,39] The circles (○), the triangles (△), and the squares (□) come from polymeric, one-dimensional, and bridging diamond core structures, respectively. The black plots (●, ▲, ■) come from the Ca(II) complexes with amide ligands.[24]

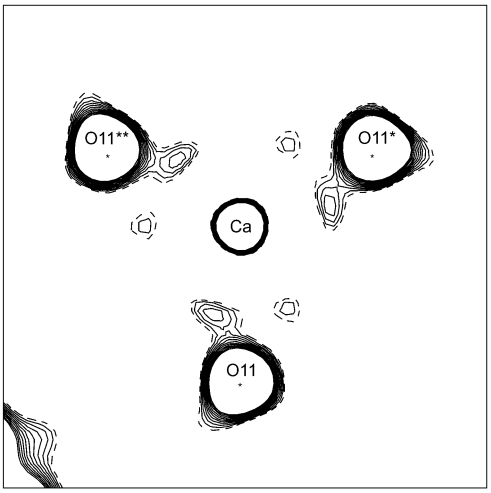

Figure 8. Fourier density map of **3** sliced between the Ca−O bond with the plane parallel to the three coordinating oxygen atoms.

Discussion

Ca−O bonds in the Ca−Phosphate Complexes. The scatter plot analyses of Ca−O bond distances and the Ca−O−P bond angles were performed to obtain information about the properties of the Ca−O(phosphate) bond. Figure 7 represents the relationship between Ca−O bond distances and the Ca−O−P bond angles of the reported Ca complexes with O_2POR, $O_2P(OH)R$ and O_3PR, $O_2P(OH)R$ ligands[16−23,38,39] involving our ones discussed in the paper. This scatter plot indicates a tendency for the Ca−O distance to be shorter when the Ca−O−P angles are getting larger, and for a brief collinear relationship to exist. A similar relationship has been also reported among well-known Ca(II)−carboxylate complexes.[40] This dependence of the Ca−O bond lengths on the angle is assumed to be due to the presence of the bonding interaction in addition to the ionic interaction. Actually, the really short Ca−O(phosphate) bond, 2.264(4) Å, is observed in our mononuclear complex, **3**, as an example. We have confirmed the bonding interaction in such a short Ca−O bond by Fourier density map of X-ray crystallographic analysis. The Fourier contour map sliced over the plane which is parallel to the coordinating three oxygen atoms is shown in Figure 8. The weak Fourier density can be found between the Ca(II) ion and the coordination O11 atom. Thus, there is presumably present the partially covalent interaction in the short Ca−O(phosphate) bond.

The covalent bonding interaction between the Ca(II) ion and the oxygen atom of phosphate groups is investigated with density functional calculations. The calculation is performed using the extracted coordinates of the coordination sphere in the crystal structure of **3**, as shown in Figure 9. The model in the absence of the Ca(II) ion is also examined, and the results of the Mulliken charge are also represented. The anionic charge on the coordinating oxygen atom is increased with the Ca ion, while the other oxygen atoms of the phosphate groups are decreased. Thus, it is indicated that the anionic charge is relatively localized on the coordinating O atom. The molecular orbitals are also presented in Figure 9. The HOMO orbital on the coordinating oxygen atoms has a slight anisotropy directed to the Ca center, which is indicative of the participation of Ca orbitals. Such a kind of anisotropy can be found in other lower level orbitals and clearly, for example, in HOMO (−3) and HOMO (−8) with C_3 symmetry. Actually, the participation of the 3p and 4d orbitals on the Ca ion is confirmed by density matrix analyses. The gross orbital population analysis shows that 0.0096% of the total electron density on the Ca ion occupies the 3d orbitals. These computational results also support the participation of the $d\pi-p\pi$ and $p\pi-p\pi$ interaction in the short Ca−O(phosphate) bond.

The d orbital participation in small covalent bonding has been proposed previously in some Ca complexes on the basis of crystallographic data or ab initio calculations. It has been suggested by an extensively short Ca−O bond distance (2.197 Å) in a Ca−phenolate complex with a nearly liner Ca−O−C(aryl) bond angle (173.9°) that the d or p orbitals of the Ca(II) ion are involved in the Ca−O bonds with the phenolate ligand.[41] The computational experiments on CaX_2 ($X = F, Cl, Br, I, CH_3, NH_2$) lead us to conclude that both core polarization and d orbital participation in small covalent bonding contributions (influence of valence shell) control the bending structures.[42−45] The previous research also establishes the presence of some covalent character in the Ca−O(phosphate) bonds.

Functions of the Hydrogen Bonding between the Amide NH and the Oxygen Atoms of Phosphate. The combined X-ray, ^1H NMR, and IR results indicate that the NH···O hydrogen bond between the amide NH and the phosphate was not formed in the acid state and a weak one exists in

(38) Catti, M.; Ferraris, G. *Acta Crystallogr.* **1980**, *B36*, 254−259.
(39) Curry, N. A.; Jones, D. W. *J. Chem. Soc. A* **1971**, 3725−3729.
(40) Einspahr, H.; Bugg, C. E. *Acta Crystallogr.* **1981**, *B37*, 1044−1052.
(41) Tesh, K. F.; Hamusa, T. P.; Huffman, J. C.; Huffman, C. J. *Inorg. Chem.* **1992**, *31*, 5572−5579.
(42) Kaupp, M.; Schleyer, R. v. R.; Stolll, H.; Preuss, H. *J. Chem. Phys.* **1991**, *94* (2), 1360−1366.
(43) Kaupp, M.; Schleyer, R. v. R. *J. Am. Chem. Soc.* **1992**, *114*, 491−497.
(44) Kaupp, M.; Schleyer, R. v. R. *J. Am. Chem. Soc.* **1993**, *115*, 11202−11208.
(45) Mösges, G.; Hampel, F.; Kaupp, M.; Schleyer, R. v. R. *J. Am. Chem. Soc.* **1992**, *114*, 10880−10889.

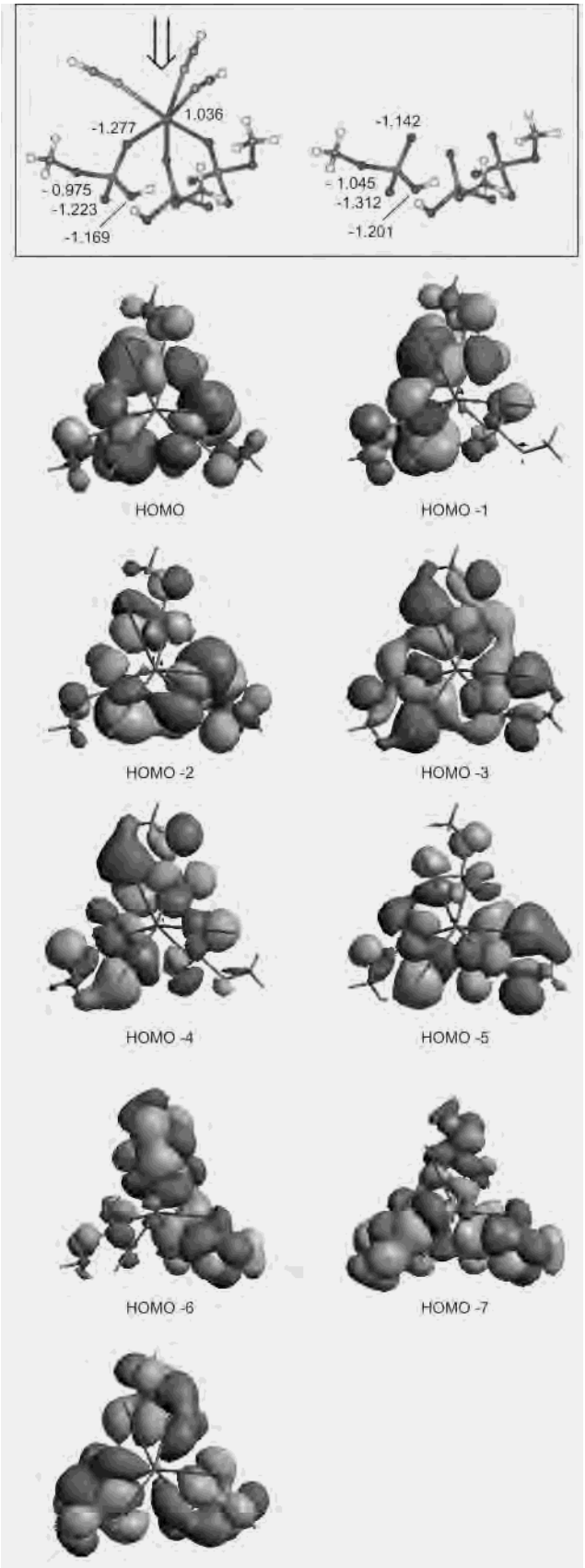

Figure 9. Constructed models with and without Ca ion for the DFT calculations are shown in the upper square. The coordinates of them are based on the crystal structure of **3**. The Mulliken charges of selected atoms are also represented. The molecular orbital plots of the Ca−phosphate complex model are shown in the bottom structures. The view is from the direction of the arrow.

the phosphate monoanion state, while a strong one is found in the phosphate dianion state. The difference in strength of NH···O hydrogen bonds between these states originates from the difference in the two pK_a values, pK_{a1} (ca. 2) and pK_{a2} (ca. 7), of dihydrogen phosphate ligands. The first deprotonation of the PO−H^1 gives the corresponding stabilized anion, and the next PO−H^2 produces a more basic anion. Previously, we reported that the strength of the NH···O hydrogen bonds between the amide NH and the oxygen atom of an oxo-acid are correlated with their pK_a values.[46] In that report, we investigated the strength of the NH···O hydrogen bonds in 2,6-(^{t}BuCONH)$_2$C$_6$H$_3$COOH, in 2-(^{t}BuCONH)$_2$C$_6$H$_4$-SO$_3$H, and in their anion states. The sulfonic acid, ArSO$_3$H, has a very low pK_a value (ca. −1) because its anion ArSO$_3^-$ has a strong conjugation stabilizing the anionic charge. The NH···O hydrogen bonds between the amide NH and the oxygen atoms of sulfonate are very weak in the ArSO$_3^-$ state.[46] The NH···O hydrogen bonds to the oxygen atom in the ArCOO$^-$ state are much stronger than those in the ArSO$_3^-$ state. These results support that the stronger NH···O hydrogen bonds are formed in the phosphate dianion having higher basicity.

The NH···O hydrogen bonds can localize the anion charge of phosphate and decrease the basicity of the anion; that is, the pK_a values become lower. The pK_{a1} and pK_{a2} values of 2,6-(Ph$_3$CCONH)$_2$C$_6$H$_3$OPO$_3$H$_2$ (**1**) in 50% aqueous THF solution are 3.3 and 7.9, respectively. The pK_{a1} and pK_{a2} values of the ^{i}Pr-substituted ligand, 2,6-^{i}Pr−C$_6$H$_3$OPO$_3$H$_2$, without an NH···O hydrogen bond are 3.6 and 8.0, respectively, under the same conditions. This result suggests that the deprotonation of the P−OH^1 and P−OH^2 in hydrogen phosphate **1** is promoted by NH···O hydrogen bonds.

The lowering of the pK_a values by the hydrogen bonds contributes to the increase of stability constant of Ca(II) ions. Our hydrogen-bonded phosphate ligand shows a smaller pK_a value, and our ligand exchange experiments monitored by ^{1}H NMR spectra indicate that the hydrogen bonds to the coordinating phosphate group prevent the Ca−O bond from dissociation and force Ca−O bonding. Similar effects of the NH···O hydrogen bonds are observed in a Ca(II)−carboxylate complex.[47] Our results strongly indicate that the NH···O hydrogen bonds from the amide NH localize the anion charge on coordinating phosphate groups, preventing the Ca−O bond from dissociation via lowering the pK_a values.

Construction of Novel Ca(II)−Phosphate Structures with Bulky Amide Ligands. The bulky phosphate ligand containing amide groups presented here interrupts the polymerization of Ca(II) ions and gives homoleptic mononuclear Ca(II) complex. Except for our Ca(II) complexes described here, all of the reported Ca(II)−O$_3$POR and −O$_3$-PR complexes have polymeric structures.[16−23,38,39] In the phosphate monoanion state, the reported Ca(II) complexes have the layered or one-dimensional chain structure involving

(46) Onoda, A.; Yamada, Y.; Doi, M.; Okamura, T.; Ueyama, N. *Inorg. Chem.* **2001**, *40*, 516−521.
(47) Yamada, Y.; Onoda, A.; Ueyama, N.; Okamura, T.; Adachi, H.; Nakamura, A. To be submitted.

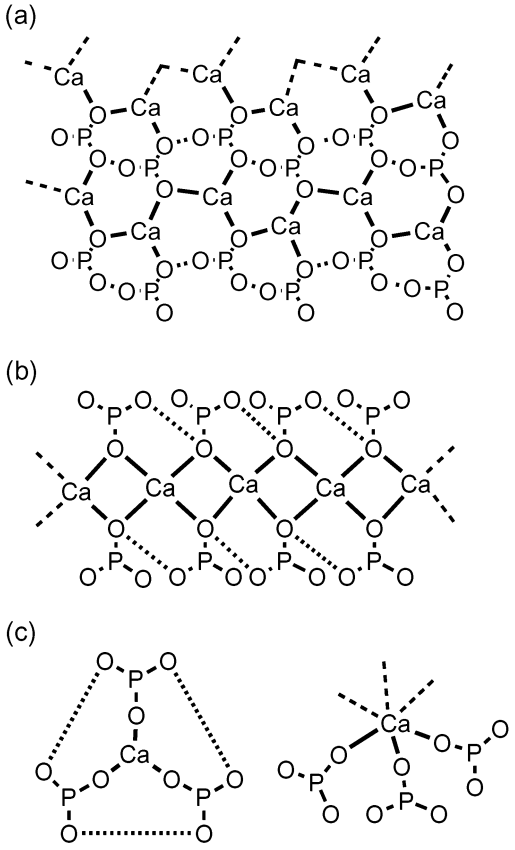

Figure 10. Schematic representation of P−OH···O−P hydrogen bonds in the Ca(II)−phosphate or phosphonate monoanion complexes shown as (a) a layered structure, (b) a one-dimensional chain, and (c) a mononuclear structure. Dashed lines refer to P−OH···O−P hydrogen bonds.

the intermolecular P−OH···O═P hydrogen bonds as represented in Figure 10a,b.[16,21] The reported phosphate dianion complexes also give polymeric structures (Figure 11a). Our bulky amide ligand prevents the polymeric coordination of the phosphate groups and the formation of infinite intramolecular P−OH···O═P hydrogen bonds. Thus, we can successfully synthesize a mononuclear Ca(II) complex both in phosphate monoanion (Figure 10c) and in the dianion (Figure 11b). High bulkiness of triphenylacylamino ligand interferes with the bridging coordination of phosphate to give monodentate coordination with *unsymmetric* ligand positions as seen for **3** and **4**. Consequently, a rational design of the strategically oriented bulky amide ligands is an intriguing approach to constructing unusual Ca(II)−phosphate structures.

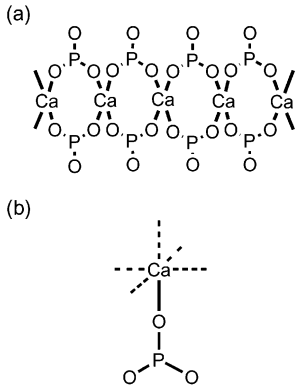

Figure 11. Schematic representation of (a) the one-dimensional structure of the reported Ca(II) complexes and (b) the mononuclear Ca(II) core with *unsymmetric* ligand coordination.

Conclusions

Novel mononuclear Ca(II) complexes with the phosphate monoanion and the dianion ligands with the bulky amide groups were structurally and spectroscopically characterized. The NH···O hydrogen bond between the amide NH and the oxygen atoms of phosphate serves as an effective probe to estimate the basicity of the O^- anion on the phosphate group. These NH···O hydrogen bonds can decrease the pK_a values of coordinating phosphate groups, followed by preventing the Ca−O bond from dissociation. Our results indicate that the NH···O hydrogen bonds are involved in regulation of the formation of the Ca−O bonds in phosphotransferase. The trends of the Ca−O−P geometry are investigated, and the Fourier density analysis and DFT calculations reveal the partial degree of covalency in the Ca−O(phosphate) bonds that is present. In conclusion, the mononuclear Ca(II) complexes using strategically designed bulky amide ligands clarify the functional role of the NH···O hydrogen bonds in coordinating the phosphate groups.

Acknowledgment. Support of this work by JSPS Fellowships [for A.O.: Grant 2306(1999-2002)] and a Grant-in-Aid for Scientific Research on Priority Area (A) (Grant 10146231) from the Ministry of Education, Science, Sports and Culture, Japan, is gratefully acknowledged.

Supporting Information Available: X-ray crystallographic data, in CIF format. This material is available free of charge via the Internet at http://pubs.acs.org.

IC010570F